



X International Conference on Structural Dynamics, EURODYN 2017

Long-term stochastic extreme response analysis of floating bridges

Finn-Idar Grøtta Giske^{a,b,*}, Bernt Johan Leira^a, Ole Øiseth^c

^aDepartment of Marine Technology, NTNU, 7491 Trondheim, Norway

^bMulticonsult, Nedre Skøyen vei 2, 0213 Oslo, Norway

^cDepartment of Structural Engineering, NTNU, 7491 Trondheim, Norway

Abstract

For the assessment of extreme responses needed in design of marine structures, a full long-term analysis is recognized as the most accurate approach. However, due to the very large number of structural response analyses traditionally needed for this approach, the computational effort is usually considered to increase above acceptable levels for complex structures such as floating bridges. This paper shows that the first and second order reliability methods (FORM and SORM) found in connection with structural reliability analysis can be used in an inverse manner to efficiently obtain approximate solutions for the full long-term extreme response of structures subjected to environmental loads, and this is demonstrated for floating bridges. Very accurate results are obtained using a limited number of short-term response calculations, and by applying a fast calculation method for the short-term stochastic response, full long-term extreme responses are calculated for two different pontoon floating bridges.

© 2017 The Authors. Published by Elsevier Ltd.

Peer-review under responsibility of the organizing committee of EURODYN 2017.

Keywords: floating bridge, pontoon, extreme response, long-term response, stochastic processes, IFORM, ISORM

1. Introduction

Fjord crossing technology is currently a very relevant research topic in Norway, and floating bridges are among the structures that are considered. The design of more extreme yet reliable fjord crossing structures requires development of the methods for long-term stochastic response analysis. Even though full long-term extreme response analysis is recognized as the most accurate approach [1], the computational cost associated with a large number of short-term response calculations is usually too large for complex systems, and simplified approaches such as the environmental contour methods are used [2].

Recently, efforts have been made to reduce the number of required short-term calculations needed for a full long-term extreme response analysis in the general context of marine structures [3–5]. In addition, the short-term response analyses can be made more efficient using the method described in [6,7]. In the present paper it is shown how these recent developments can be used to perform full long-term extreme response analyses for pontoon floating bridges.

* Corresponding author.

E-mail address: finn.i.giske@ntnu.no

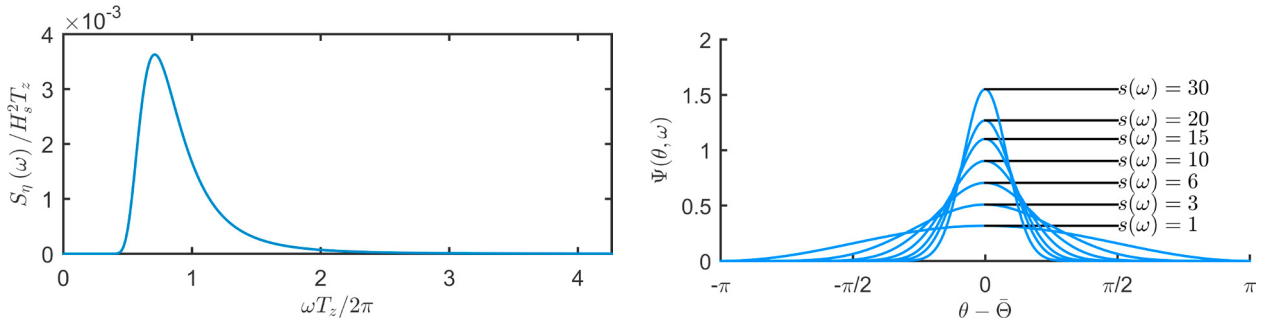


Fig. 1. (a) the generalized Pierson-Moskowitz spectrum; (b) the *cos-2s* spreading function.

2. Short-term response

2.1. Stochastic modelling of waves

For a short-term period of duration \tilde{T} , the sea elevation is modelled as a homogeneous and stationary stochastic process with zero mean. The sea elevation process is denoted $\eta(x, y, t)$, where x, y are the spatial variables and t is the time variable. Assuming linear wave theory, the wave number $\kappa(\omega)$ is a function of angular frequency defined by the dispersion relation $\omega^2 = \kappa g \tanh(\kappa d)$, and the cross-spectral density between the wave elevation at two points (x_m, y_m) and (x_n, y_n) can be expressed in terms of a one-dimensional wave spectrum $S_\eta(\omega)$ and a spreading function $\Psi(\theta, \omega)$ as

$$S_{mn}(\omega) = S_\eta(\omega) \int_{-\pi}^{\pi} \Psi(\theta, \omega) e^{-i\kappa(\omega)(\Delta x \cos \theta + \Delta y \sin \theta)} d\theta.$$

Here $\Delta x = x_m - x_n$ and $\Delta y = y_m - y_n$ are the spatial separations of the points. For details we refer to [7].

The sea elevation is further assumed to be a Gaussian process which means that the cross-spectral densities provide a complete description of the process. Hence the wave situation is completely described by the wave spectrum $S_\eta(\omega)$ and the spreading function $\Psi(\theta, \omega)$. Various theoretical models given in terms of environmental parameters exist in the literature [8,9]. In this paper we use the generalized Pierson-Moskowitz spectrum [9] given by

$$S_\eta(\omega) = \frac{H_s^2 T_z}{8\pi^2} \left(\frac{\omega T_z}{2\pi}\right)^{-5} \exp\left\{-\frac{1}{\pi} \left(\frac{\omega T_z}{2\pi}\right)^{-4}\right\},$$

where H_s is the significant wave height and T_z is the zero-crossing period. The spreading function is of the *cos-2s* type, defined by a mean wave direction $\bar{\Theta}$ relative to the x -axis and an ω -dependent spreading parameter $s(\omega)$ as

$$\Psi(\theta, \omega) = \frac{2^{2s(\omega)} \Gamma^2(s(\omega) + 1)}{2\pi \Gamma(2s(\omega) + 1)} \left(\cos^2 \frac{\theta - \bar{\Theta}}{2}\right)^{s(\omega)},$$

where $\Gamma(\cdot)$ is the gamma function. Fig. 1 shows the wave spectrum $S_\eta(\omega)$ plotted in the nondimensional scale $\omega T_z / 2\pi$, and the spreading function is shown for different values of $s(\omega)$. In this paper we have used a constant $s(\omega) = 10$, but it could equally well be defined ω -dependent. Using these models the short-term wave situation is completely described by the vector of environmental parameters $\mathbf{W} = [H_s, T_z, \bar{\Theta}]$.

2.2. Stochastic modelling of first order wave loads on pontoon bridges

In this paper we use as examples two different pontoon floating bridges: The Bergsøysund bridge with seven pontoons and a span of 913 m, located on the north-west coast of Norway, and a chained floating bridge [10] with 20 pontoons and a span of 4 km which is a new floating bridge concept. In Fig. 2 an illustration of the chained floating bridge is given, and the pontoon arrangement of the Bergsøysund bridge is displayed.

For pontoon floating bridges the structure will experience wave loads only where the pontoons are located. Considering the pontoons as rigid bodies, the bridge will experience loads in six degrees of freedom (dofs) from each

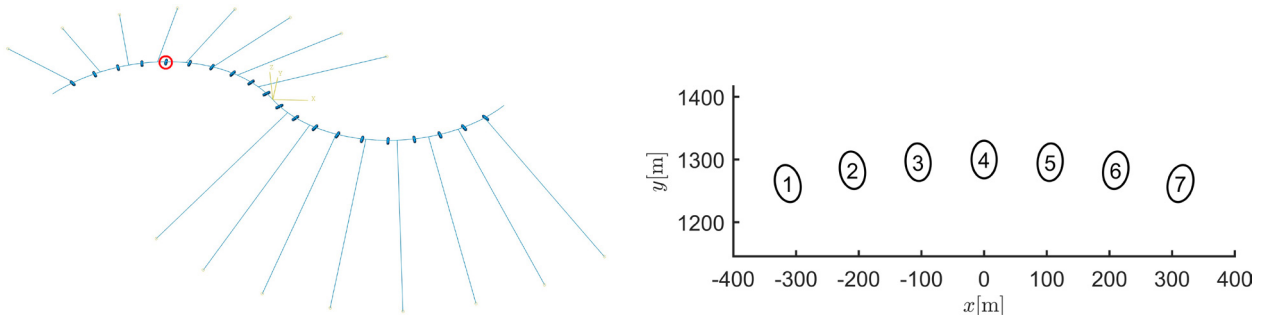


Fig. 2. (a) illustration of the finite element model for the chained floating bridge. Pontoon number 5 is highlighted with a red circle; (b) the pontoon arrangement for the Bergsøysund floating bridge.

pontoon, three translational dofs and three rotational dofs. Thus, for a bridge with N pontoons we have loading in $6N$ dofs, and we can define a wave excitation load vector $\mathbf{q}(t) = [\mathbf{q}_1(t), \mathbf{q}_2(t), \dots, \mathbf{q}_N(t)]$, where $\mathbf{q}_m(t)$ denotes the 6-element load vector of pontoon number m . The individual components of the load vector $\mathbf{q}(t)$ can be denoted by $q_\mu(t)$, assigning to each dof a global index $\mu \in \{1, 2, \dots, 6N\}$.

Consider pontoon m with a local coordinate system (\tilde{x}, \tilde{y}) , which is located with its origin at the point (x_m, y_m) and rotated counterclockwise with an angle α_m relative to the global coordinate system (x, y) as shown in Fig. 3a. The wave excitation loads due to a regular wave with angular frequency ω in the direction $\tilde{\beta}$ relative to the \tilde{x} -axis of the pontoon can be computed using linear potential theory software such as WADAM [11]. The loads are then reported in terms of the 6-element complex transfer function vector $\mathbf{f}_m(\tilde{\beta}, \omega)$. Considering only first order wave loads, the wave excitation load process $\mathbf{q}_m(t)$ corresponding to the wave elevation process $\eta(x, y, t)$ can be obtained by superposition of loads from regular waves. This results in a stationary Gaussian load process $\mathbf{q}(t)$ with zero mean and a $6N$ -by- $6N$ cross-spectral density matrix $\mathbf{S}_q(\omega)$ whose elements are given by

$$S_{q_\mu q_\nu}(\omega) = S_\eta(\omega) \int_{-\pi}^{\pi} \Psi(\theta, \omega) f_\mu(\theta - \alpha_m, \omega) \overline{f_\nu(\theta - \alpha_n, \omega)} e^{-i\kappa(\omega)(\Delta x \cos \theta + \Delta y \sin \theta)} d\theta, \tag{1}$$

where the overline denotes complex conjugation. Here $f_\mu(\tilde{\beta}, \omega)$ is the μ -th component of the total transfer function vector $\mathbf{f}(\tilde{\beta}, \omega) = [f_1(\tilde{\beta}, \omega), f_2(\tilde{\beta}, \omega), \dots, f_N(\tilde{\beta}, \omega)]$, i.e. the complex transfer function of the dof μ .

A method for efficient calculation of the cross-spectral density matrix $\mathbf{S}_q(\omega)$ based on the expression Eqn. (1) is given in [6,7]. In [7] the derivation of the cross-spectral densities is also explained in more detail.

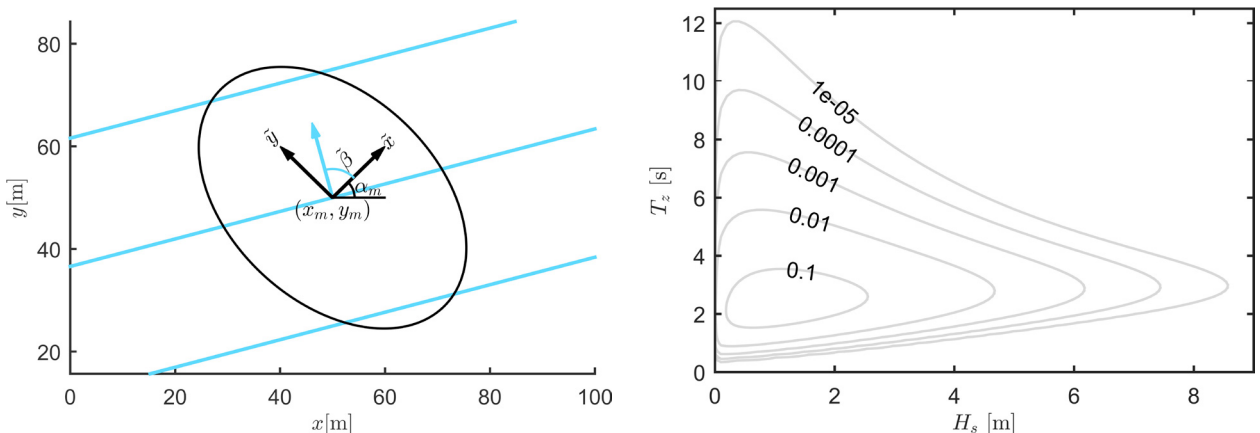


Fig. 3. (a) local coordinate system of a pontoon; (b) the joint PDF $f_w(\mathbf{w}) = f_{H_s, T_z}(h_s, t_z)$ illustrated by its isoprobability contours.

2.3. Stochastic response of floating bridges

For a floating bridge with N pontoons, let $\mathbf{u}(t)$ denote the displacement vector corresponding to the same dofs as the load vector $\mathbf{q}(t)$. This means that $\mathbf{u}(t)$ gives the displacements and rotations of the bridge at the locations of the pontoons. Now the frequency domain representations of $\mathbf{u}(t)$ and $\mathbf{q}(t)$ given by their Fourier transforms are denoted $\hat{\mathbf{u}}(\omega)$ and $\hat{\mathbf{q}}(\omega)$ respectively, and the equation of motion can be written in the frequency domain as

$$\left(-\omega^2(\mathbf{M}_s + \mathbf{M}_h(\omega)) + i\omega(\mathbf{C}_s + \mathbf{C}_h(\omega)) + (\mathbf{K}_s + \mathbf{K}_h)\right)\hat{\mathbf{u}}(\omega) = \hat{\mathbf{q}}(\omega). \quad (2)$$

Here \mathbf{M}_s , \mathbf{C}_s and \mathbf{K}_s are structural mass, damping and stiffness matrices, which can be obtained from a finite element model of the bridge structure. The frequency dependent hydrodynamic mass and damping matrices $\mathbf{M}_h(\omega)$ and $\mathbf{C}_h(\omega)$, as well as the hydrostatic stiffness matrix \mathbf{K}_h , can be obtained by assembling linear potential theory results for the individual pontoons. The details on establishing the equation of motion Eqn. (2) can be found in [12].

The equation of motion Eqn. (2) can be solved in the frequency domain by matrix inversion, giving

$$\hat{\mathbf{u}}(\omega) = \mathbf{H}(\omega)\hat{\mathbf{q}}(\omega), \quad (3)$$

where $\mathbf{H}(\omega) = \left(-\omega^2(\mathbf{M}_s + \mathbf{M}_h(\omega)) + i\omega(\mathbf{C}_s + \mathbf{C}_h(\omega)) + (\mathbf{K}_s + \mathbf{K}_h)\right)^{-1}$ is the load to response transfer function matrix. The relation Eqn. (3) implies that $\mathbf{u}(t)$ will be the response of a linear and time-invariant dynamical system, from which it follows that $\mathbf{u}(t)$ is a stationary Gaussian process with zero mean whenever $\mathbf{q}(t)$ is. Hence, the response process $\mathbf{u}(t)$ will be fully characterized by its cross-spectral density matrix, which according to [1] is given by

$$\mathbf{S}_u(\omega) = \mathbf{H}(\omega)\mathbf{S}_q(\omega)\mathbf{H}(\omega)^H,$$

where $[\cdot]^H$ denotes conjugate transpose. This is referred to as the power spectral density method [12,13].

2.4. Short-term extreme value distribution

We now consider one component process $u_\mu(t)$ of the response vector process $\mathbf{u}(t)$. This will be the displacement in the dof μ , so if for instance $\mu = 8$ then $u_\mu(t)$ will be the displacement in the \tilde{y} -direction (see Fig. 3a) of pontoon number 2, and relative to the bridges in Fig. 2 this is the horizontal transverse direction. Now the maximal value of $u_\mu(t)$ during a short-term period with given environmental variables \mathbf{W} will be a random variable, we denote it by $\tilde{R}|\mathbf{W}$, and we seek its cumulative distribution function (CDF) $F_{\tilde{R}|\mathbf{W}}(r|\mathbf{w}) = \text{Prob}[\tilde{R} \leq r|\mathbf{W} = \mathbf{w}] = \text{Prob}[\tilde{R} \leq r|H_s = h_s, T_z = t_z, \bar{\Theta} = \bar{\theta}]$.

Since $\mathbf{u}(t)$ is stationary and Gaussian with zero mean, so will $u_\mu(t)$. As explained in detail in [1], the short-term extreme value distribution $F_{\tilde{R}|\mathbf{W}}(r|\mathbf{w})$ can be found by assuming independent upcrossings of high levels r as

$$F_{\tilde{R}|\mathbf{W}}(r|\mathbf{w}) = \exp\left\{-\frac{\tilde{T}}{2\pi} \sqrt{\frac{m_2(\mathbf{w})}{m_0(\mathbf{w})}} \exp\left\{-\frac{r^2}{2m_0(\mathbf{w})}\right\}\right\}, \quad (4)$$

which holds for reasonably large values of r . The i -th moment $m_i(\mathbf{w})$ of the response spectrum of $u_\mu(t)$ is defined as $m_i(\mathbf{w}) = \int_0^\infty \omega^i S_{u_\mu u_\mu}(\omega) d\omega$. Here $S_{u_\mu u_\mu}(\omega)$ is the auto-spectral density of $u_\mu(t)$, i.e. the μ -th element along the diagonal of the cross-spectral density matrix $\mathbf{S}_u(\omega)$. Note that $\mathbf{u}(t)$ and $\mathbf{S}_u(\omega)$ depend on the environmental parameters \mathbf{w} , though not written explicitly.

It should be noted that although Eqn. (1) and thereby Eqn. (4) are based on the assumption of homogeneity, which may be questioned for floating bridge applications, the general method presented in this paper is readily used along with other ways of calculating the short-term CDF $F_{\tilde{R}|\mathbf{W}}(r|\mathbf{w})$. The only required assumption is that the response process can be approximated as stationary for some short-term period \tilde{T} .

3. Long-term extreme response

3.1. The long-term extreme response model

For the modelling of long-term extreme response of marine structures, the long-term situation is commonly considered as a collection of \tilde{N} short-term states, each of duration \tilde{T} . During each short-term state the environmental

processes are assumed stationary and defined by a set of n environmental parameters $\mathbf{W} = [W_1, W_2, \dots, W_n]$, whose joint probability density function (PDF) is $f_{\mathbf{W}}(\mathbf{w})$. In this paper we only consider the stochastic response of floating bridges due to wave loads, so the short-term period is $\tilde{T} = 3\text{h}$ and the environmental parameters are $\mathbf{W} = [H_s, T_z, \bar{\Theta}]$.

The long-term CDF of the short-term extreme value is denoted $F_{\tilde{R}}(r)$, and gives the distribution of the largest response value \tilde{R} during an arbitrarily chosen short-term condition. This can be obtained as an average of the short-term CDFs $F_{\tilde{R}|\mathbf{W}}(r|\mathbf{w})$ weighted by the distribution $f_{\mathbf{W}}(\mathbf{w})$ of the environmental parameters. Basic to the concept of long-term statistics is the assumption of ergodicity, and in order to make any estimation of $f_{\mathbf{W}}(\mathbf{w})$ the ergodicity assumption is required for the environmental parameters [14]. Hence $F_{\tilde{R}}(r)$ should be expressed as an ergodic average [1,14]. This yields the long-term extreme response formulation

$$F_{\tilde{R}}(r) = \exp \left\{ \int_{\mathbf{w}} (\ln F_{\tilde{R}|\mathbf{W}}(r|\mathbf{w})) f_{\mathbf{W}}(\mathbf{w}) d\mathbf{w} \right\}. \tag{5}$$

3.2. Calculation of the M -year extreme response using inverse reliability methods

From the long-term CDF $F_{\tilde{R}}(r)$, characteristic values of the extreme response can be obtained. In this paper we consider the M -year extreme response r_M , defined as the response level that is exceeded on average once every M years. When the short-term period is $\tilde{T} = 3\text{h}$ there are $M \cdot 365 \cdot 8 = 2920M$ short-term periods in M years. This means that the probability of \tilde{R} exceeding r_M is $1/2920M$, and r_M can be found by requiring $1 - F_{\tilde{R}}(r_M) = 1/2920M$.

Using a similar approach as in [4,5], the long-term CDF in Eqn. (5) can be rewritten in an approximate manner as

$$F_{\tilde{R}}(r) \approx \exp \left\{ -C \int_{G_r(\mathbf{v}) \leq 0} f_{\mathbf{V}}(\mathbf{v}) d\mathbf{v} \right\}, \tag{6}$$

where $\mathbf{V} = [\mathbf{W}, Y]$ is a random vector containing the environmental variables \mathbf{W} and a random variable Y defined by a conditional CDF $F_{Y|\mathbf{W}}(y|\mathbf{w}) = \max \left\{ 1 + \frac{1}{C} \ln \left(F_{\tilde{R}|\mathbf{W}}(y|\mathbf{w}) \right), 0 \right\}$. The function $G_r(\mathbf{v})$ is the so-called limit state function. In [4] $C = 1$ is used, but a larger value of C can be used to improve the accuracy of the approximation. Now the integral in Eqn. (6) can be solved using the first order reliability method (FORM) or the second order reliability method (SORM). The M -year extreme response r_M can be obtained by using these reliability methods inversely as shown in [4] for inverse FORM (IFORM) and in [5] for inverse SORM (ISORM).

4. Results and discussion

In order to demonstrate the methods described in this paper, short-term response models were established for the Bergsøysund bridge and the chained floating bridge as described in Section 2, and the IFORM and ISORM methods were implemented in MATLAB. The response processes considered here are the horizontal transverse displacements of pontoon 4 ($u_{20}(t)$) for the Bergsøysund bridge and pontoon 5 ($u_{26}(t)$) for the chained floating bridge, see Fig. 2.

Using a deterministic mean wave direction along the negative y -axis, $\bar{\Theta} = \bar{\theta} = -\frac{\pi}{2}$, we obtain a 2D environmental model defined by the parameters $\mathbf{W} = [H_s, T_z]$. The joint PDF $f_{\mathbf{W}}(\mathbf{w}) = f_{H_s, T_z}(h_s, t_z)$ is illustrated in Fig. 3b. Since it is only H_s and T_z that change between different environmental states, it is only the wave spectrum $S_{\eta}(\omega)$ that must be computed repeatedly, while the integral in Eqn. (1) must be computed only once for each combination of dofs μ and ν . This results in very efficient short-term response calculations for the 2D environmental model.

We also consider a 3D environmental model where $\mathbf{W} = [H_s, T_z, \bar{\Theta}]$. The mean wave direction $\bar{\Theta}$ is then assumed to be uniformly distributed between $-\pi$ and π , and independent of H_s and T_z . Thus the PDF of the environmental parameters becomes $f_{\mathbf{W}}(\mathbf{w}) = f_{H_s, T_z}(h_s, t_z) f_{\bar{\Theta}}(\bar{\theta})$, where $f_{H_s, T_z}(h_s, t_z)$ is the same as before and $f_{\bar{\Theta}}(\bar{\theta})$ is a uniform PDF. Note that the environmental models do not correspond to a specific site, but serve to illustrate the general methodology.

The 100-year extreme response values r_M , $M = 100$, for the selected dofs of the two bridges were calculated using the inverse reliability methods. For comparison, the method described in [3] using IFORM and importance sampling Monte Carlo simulation (ISMCS) was also applied. The extreme responses are given in Tab. 1 for the 2D and 3D environmental models, along with the number of required short-term response calculations n_{st} . For the ISMCS method r_M is reported as $\bar{r} \pm s$, where \bar{r} and s are the sample mean and standard deviation obtained when 100 independent runs of the method were performed, with each run requiring n_{st} short-term response calculations. The efficiency of the 2D

Table 1. The 100-year extreme response r_M , $M = 100$, calculated using the different methods. The number of required short-term response calculations n_{st} is also given for each of the methods.

Models	IFORM		ISORM, $C=1$		ISORM, $C=10^6$		ISMCS		Full integration	
	r_M [m]	n_{st}	r_M [m]	n_{st}	r_M [m]	n_{st}	r_M [m]	n_{st}	r_M [m]	n_{st}
Bergs., 2D	5.77	90	5.54	159	5.62	85	5.61±0.09	140	5.62	39597
Chained, 2D	4.67	66	4.24	151	4.81	133	4.80±0.10	116	4.82	39597
Bergs., 3D	5.68	105	5.05	179	5.11	136	5.07±0.14	155		
Chained, 3D	4.52	65	3.46	195	4.24	195	4.50±0.22	115		

environmental model allowed for full numerical integration of the long-term CDF in Eqn. (5), and the corresponding exact extreme response values are therefore given in this case.

Comparing the results for the 2D environmental model, we see that all methods give good estimates of the 100-year extreme response. The ISORM method with $C = 10^6$ gives very accurate results. This choice for C was somewhat arbitrary, and further work should be carried out to investigate the effect of this parameter. The results for the 3D environmental model are consistent, indicating that valid results are obtained also in this case. Finally, it should be mentioned that even though IFORM and ISORM perform very well for this example, these methods do have some known difficulties. Nevertheless, the demonstrated methods could still provide valuable estimates.

5. Conclusions

It has been shown how IFORM and ISORM can be used to perform full long-term extreme response analyses for complex structures such as floating bridges. The methods provide good accuracy using only a reasonable amount of short-term response calculations.

Acknowledgements

The authors are grateful for grants which are provided by Multiconsult ASA and the Research Council of Norway. We would also like to thank Knut Andreas Kvåle for the finite element modelling of the bridges.

References

- [1] A. Naess, T. Moan, Stochastic dynamics of marine structures, Cambridge University Press, Cambridge, 2012.
- [2] S. Haver, G. Kleiven, Environmental contour lines for design purposes: why and when?, ASME Conf. Proc. 2004 (2004) 337–345.
- [3] L. Sagrilo, A. Naess, A. Doria, On the long-term response of marine structures, Appl Ocean Res 33 (2011) 208–214.
- [4] F.-I. G. Giske, B. J. Leira, O. Øiseth, Full long-term extreme response analysis of marine structures using inverse FORM, 2017. Preprint submitted to Prob. Eng. Mech..
- [5] F.-I. G. Giske, B. J. Leira, O. Øiseth, Long-term extreme response analysis of marine structures using inverse SORM, 2017. Paper submitted to OMAE2017.
- [6] F.-I. G. Giske, B. J. Leira, O. Øiseth, Stochastic Modelling of Wave Loads on Floating Bridges : Efficient Calculation of Cross-Spectral Densities, in: 19th Congr. IABSE, Challenges Des. Constr. an Innov. Sustain. Built Environ., September, 2016, pp. 48–56.
- [7] F.-I. G. Giske, B. J. Leira, O. Øiseth, Efficient computation of cross-spectral densities in the stochastic modelling of waves and wave loads, Appl. Ocean Res. (2017).
- [8] D. Hauser, K. Kahma, H. Krogstad, Measuring and analysing the directional spectra of ocean waves, Luxembourg: Publications Office of the European Union, 2005.
- [9] C. T. Stansberg, G. Contento, S. W. Hong, M. Irani, S. Ishida, R. Mercier, Y. Wang, J. Wolfram, J. Chaplin, D. Kriebel, The specialist committee on waves final report and recommendations to the 23rd ITTC, in: Proceedings of the 23rd ITTC, 2002, pp. 505–736.
- [10] B. Opgård, F. Allievi, Chained Floating Bridge, in: IABSE Symp. Rep., volume 102, IABSE, 2014, pp. 1236–1243.
- [11] DNV, SESAM User Manual Wadam Wave Analysis by Diffraction and Morison Theory, 2014.
- [12] K. A. Kvåle, R. Sigbjørnsson, O. Øiseth, Modelling the stochastic dynamic behaviour of a pontoon bridge: A case study, Comput Struct 165 (2016) 123–135.
- [13] K. A. Kvåle, O. Øiseth, R. Sigbjørnsson, Modelling of the stochastic dynamic behaviour of the Bergsøysund Bridge: an application of the power spectral density method, in: IX International Conference on Structural Dynamics, EURODDYN 2014, volume 1, 2014, pp. 2921–2928.
- [14] A. Naess, Technical note: On the long-term statistics of extremes, Appl. Ocean Res. 6 (1984) 227–228.